This article has been accepted for publication in a future issue of this journal, but has not been fully edited. Content may change prior to final publication. Citation information: DOI 10.1109/TSG.2020.3020466, IEEE Transactions on Smart Grid

Game Theoretic-Based Distributed Charging Strategy for PEVs in A Smart Charging Station

Yanni Wan, *Student Member, IEEE*, Jiahu Qin, *Senior Member, IEEE*, Fangyuan Li, *Member, IEEE*, Xinghuo Yu, *Fellow, IEEE*, and Yu Kang, *Senior Member, IEEE*

***Abstract*—This paper investigates the charging problem of plug-in electric vehicles (PEVs) in a smart charging station (SCS) under a new interaction mechanism that allows the interactions among PEVs. The target is to coordinate the charging strategies of all PEVs such that the energy cost of SCS is minimized without compromising a set of constraints for PEVs and SCS. To this end, we first construct a non-cooperative game framework, in which each player (i.e., PEV) expects to minimize its cost by choosing the optimal charging strategy over the entire charging horizon. Then, the existence and optimality of Nash equilibrium (NE) for the formulated non-cooperative game is provided. Moreover, to find the unique generalized Nash equilibrium (GNE), we propose a distributed GNE-seeking algorithm based on the Newton fixed-point method. And a fast alternating direction multiplier method (fast-ADMM) framework is applied to determine the best response of PEVs. The convergence of the proposed distributed GNE-seeking algorithm and PEVs' best response are also provided with theoretical analysis. Simulations are presented at last to validate the effectiveness of the proposed algorithm.**

***Index Terms*—Plug-in electric vehicle (PEV), interaction mechanism, non-cooperative game, charging strategy.**

NOMENCLATURE

α_t, β_t	Positive price coefficients at time slot t
$\boldsymbol{\lambda}$	Lagrange multiplier vector
$\boldsymbol{\mathcal{X}}(\boldsymbol{\mathcal{X}}_n)$	Feasible charging profile set of all PEVs (PEV n)
$\boldsymbol{x}^*$	Nash equilibruim of $\mathcal{G}$
$\boldsymbol{x}_{-n}$	Charging strategies of all players except player n
$\boldsymbol{x}_n$	Charging profile of PEV n over the entire charging time horizon
$\boldsymbol{y}_n$	Feasible charging strategy for PEV n
δ	Profitability index
$\Delta\boldsymbol{x}^k$	Newton direction at k-th iteration
ϵ_1, ϵ_2	Error tolerance
$\mathcal{N}$	Set of all the PEVs
$\mathcal{T}$	Set of charging time periods
$\nabla\boldsymbol{y}_\rho(\boldsymbol{x}^k)$	Gradient of $\boldsymbol{y}_\rho(\boldsymbol{x}^k)$
$\partial M(\boldsymbol{x}^k)$	Computable generalized Jacobian of M at $\boldsymbol{x}^k$
π_n^{min}/π_n^{max}	Lower/upper battery capacity of PEV n
π_n^0/π_n^T	Initial/terminal enenrgy level of PEV n at time slot t
ρ	Regularization parameter
$\varphi_\rho(\boldsymbol{x},\boldsymbol{y})$	ρ-regularized Nikaido-Isoda (NI) function
ξ_n	Proportion of the total energy consumption of PEV n in the total aggregate load of SCS
ζ	Augmented Lagrange multiplier
$C_t(L_t)$	Energy cost of SCS at time slot t
C_{tol}	Total energy cost of SCS
C_{tol}^*	Minimun energy cost of SCS
f_n	Fees paid by the owner of PEV n
$f_n(\boldsymbol{x}_n,\boldsymbol{x}_{-n})$	Cost function of PEV n
H^k	An entry of the computable generalized Jacobian
$I_1(\boldsymbol{y})/I_2(\boldsymbol{z})$	Indicator function with repsect to $\boldsymbol{y}/\boldsymbol{z}$
$L_\zeta(\boldsymbol{y},\boldsymbol{z},\boldsymbol{\lambda})$	Augmented Lagrangian
L_t	Total aggregate load of SCS at time slot t
L_{max}	Maximum allowable load of SCS
$M(\boldsymbol{x}^*)$	Mapping system
n, m	Index of PEVs
p_t	Electricty price at time slot t
R_n	Required energy of PEV n
x_n^{max}	Rated charging power of PEV n
$x_{n,t}$	Charging power of PEV n at time slot t
z	An auxiliary vector

This work was supported in part by the National Natural Science Foundation of China under Grants 61922076, 61873252, 61725304, and 61673361, in part by the Fok Ying-Tong Education Foundation for Young Teachers in Higher Education Institutions of China under Grant 161059, and in part by the Australian Research Council Discovery Program under Grant DP200101197. *(Corresponding author: Jiahu Qin.)*

Y. Wan, J. Qin, and F. Li are with the Department of Automation, University of Science and Technology of China, Hefei 230027, China (e-mail: wanyanni@mail.ustc.edu.cn; jhqin@ustc.edu.cn; fylimas@mail.ustc.edu.cn).

X. Yu is with the School of Engineering, RMIT University, VIC 3000, Australia (e-mail: x.yu@rmit.edu.au).

Y. Kang is with the Department of Automation, State Key Laboratory of Fire Science, Institute of Advanced Technology, University of Science and Technology of China, Hefei 230027, China, and also with the Key Laboratory of Technology in Geo-Spatial Information Processing and Application Systems, Chinese Academy of Sciences, Beijing 100190, China (e-mail: kangduyu@ustc.edu.cn).

I. INTRODUCTION

Due to the advantages of energy saving and emission reduction, the PEVs have become more and more popular in smart grid and attracted increasing attention from automobile industry and governments [1], [2]. With the rapid development of PEVs, the energy structure of society is undergoing significant changes [3]. However, inappropriate charging strategies for PEVs, such as charging too many PEVs at the same time, may lead to a surge in demand or an unacceptable load peak, resulting in more energy expenditure and even grid collapse [4]. Therefore, the charging coordination for PEVs in smart grid is becoming increasingly prominent, aiming to minimize the energy cost of grid while meeting the charging needs of all PEVs and avoiding resource waste, battery overload, and grid collapse [5], [6].

One striking feature of PEVs is their ability to store electrical energy, which makes the PEVs more flexible. For example, during peak times, some PEVs can act as energy

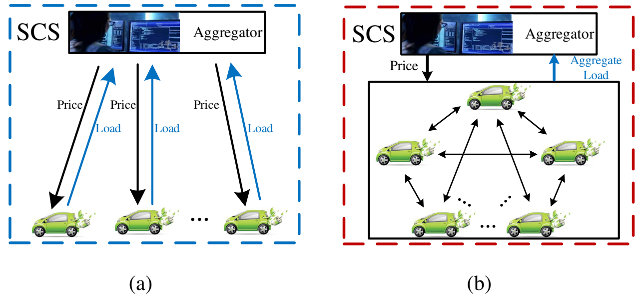

Fig. 1. (a) Traditional interaction mechanism between SCS and PEVs. (b) New interaction mechanism between SCS and PEVs combining with V2V mechanism.

suppliers rather than consumers. Recently, in addition to the common vehicle-to-grid (V2G) mechanism that allows two-way power transmission between PEVs and grid [7], some other mechanisms have been studied, such as vehicle-to-home (V2H) [8] and vehicle-to-building (V2B) [9] mechanisms. Moreover, with the development of information and communication technologies (ICTs), a new mechanism, i.e., vehicle-to-vehicle (V2V) mechanism [10], has emerged, which allows the vehicles in the same area to communicate directly with each other without the need to forward through the grid. In general, the most common communication area for PEVs is smart charging station (SCS), which is capable of controlling the behaviors of PEVs to mitigate the impact of overcharging during the peak periods [11]. The traditional interaction mechanism between SCS and PEVs (see Fig. 1(a)) requires every PEV to communicate with the aggregator embedded in SCS. Specifically, each PEV responses individually to the time-varying price determined by the aggregator by increasing/decreasing its charging request or shifting the charging request from high-price periods to low-price periods. However, due to the independence of PEVs, such traditional interaction mechanism may not be able to find the optimal charging strategy to minimize the energy cost of SCS. Therefore, we propose a new interaction mechanism (see Fig. 1(b)) combining with V2V mechanism, which first coordinates the charging strategies of all PEVs according to the time-varying price determined by the aggregator, and then transfers the aggregate load information to SCS's aggregator.

Recently, a lot of works have been devoted to study the charging problem of PEVs [7], [12]–[14]. In [12], the authors propose a time-of-use (TOU) price-based centralized charging scheduling pattern that has great benefit in reducing the charging cost and flatting the load curve. However, a new peak load may occur during the low-price periods. To address this limitation, the concept of valley-filling is introduced in [13], and a decentralized algorithm is developed to obtain the optimal charging profile that can smooth the load curve. In addition, some other works, like [7], [14], focus on the interaction between PEVs and grid. In [14], the authors adopt an unidirectional V2G mechanism to describe the interaction between PEVs and grid, which increases the adoption rate of PEVs. Then, the work [7] extends the unidirectional V2G mechanism to a bidirectional one, where the PEVs can also send the electrical energy back to the grid. However, the above-mentioned works rarely consider the strategic interactions among multiple participants in SCS.

As a result, to study the strategic interactions among multiple participants, we then focus on the game theory since it is a powerful tool for analyzing the strategic interactions among multiple decision makers to improve the system/network performance [15]. Recently, many researchers have investigated the charging coordination based on game theory [16]–[21]. In [16], a non-cooperative Stackelberg game is constructed under V2G mechanism, in which the leader (i.e., smart grid) decides the price to maximize its revenue and the followers (i.e., PEV groups) choose the charging strategies to optimize a tradeoff between individual charging benefit and associated cost. The work [17] presents a price-incentive non-cooperative game model to produce the equilibrium solutions for energy storage systems (ESSs), including the stationary and mobile batteries (i.e., PEVs). To address the network failures caused by the spatial and temporal security constraints, a distributed charging control with security constraints of distribution network is proposed in [18] based on a non-cooperative game. Another work [19] develops a distributed approach for temporal-spatial charging coordination of plug-in electric taxi fleets (PETs) by a two-stage decision process, in which the second stage devises a game-theoretical approach for PETs to select charging stations. Moreover, the authors in [20] introduce a stochastic game to study the data-driven charging strategy for PEV-based taxis. Also, a charging management with a social contribution behavior of EVs is presented in [21]. However, it is worth noting that most of the existing works mainly focus on the interactions between PEVs and grid, the potential interactions among the PEVs are rarely considered.

Motivated by the above discussions, this paper studies the charging coordination of PEVs under a new interaction mechanism (see Fig. 1(b)). The main contributions are shown below:

1) A new interaction mechanism for the PEVs and SCS is proposed. Comparing with the V2G mechanism [7], [14], [16] that considers the interaction between each PEV and aggregator/grid, the proposed mechanism combines the V2V mechanism, allowing interactions among the PEVs[1]. As a result, the flexibility of the PEVs can be fully exploited.
2) A non-cooperative game framework for PEVs charging is constructed, in which each player (i.e., PEV) chooses optimal strategy according to the strategies of all other players, so as to minimize its own cost (i.e., the payment to SCS). The existence and optimality of the NE for the formulated non-cooperative game are provided. Specifically, it is shown that the NE of the non-cooperative game is unique and minimizes the total energy cost of SCS.
3) A distributed GNE-seeking algorithm is developed based on the Newton fixed-point method. Moreover, a fast-ADMM framework is employed to determine the PEVs' best response. The convergence of the proposed dis-

[1]Since that the information exchange under the V2V mechanism is assumed to be complete and accurate rather than dishonest, the associated complexities [22] imposed by the information communication among PEVs are beyond the scope of this paper.

This article has been accepted for publication in a future issue of this journal, but has not been fully edited. Content may change prior to final publication. Citation information: DOI 10.1109/TSG.2020.3020466, IEEE Transactions on Smart Grid

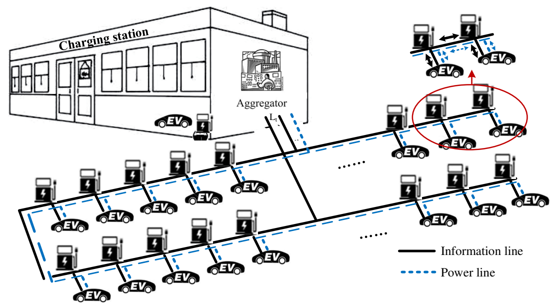

Fig. 2. Schematic diagram of a smart charging station.

tributed GNE-seeking algorithm and PEVs' best response are also presented with theoretical analysis.

The remainder of this paper is arranged as follows. The system model and problem formulation are described in Section II, followed by the non-cooperative game framework in Section III. In Section IV, the distributed GNE-seeking algorithm is proposed. The simulation results are presented in Section V and the conclusions are drawn in Section VI.

II. System Model and Problem Formulation

Consider a SCS located in residential/commercial area as shown in Fig. 2, where an aggregator sets price to coordinate the charging behavior of a finite set $\mathcal{N} = \{1, 2, \ldots, N\}$ of PEVs over the entire charging horizon $\mathcal{T} = \{1, 2, \ldots, T\}$. The PEVs actively participate in the charging coordination through charging/discharging. Denote vector $\boldsymbol{x_n} = (x_{n,1}, x_{n,2}, \ldots, x_{n,T})^T$ as the charging profile of PEV n over the charging horizon, where $x_{n,t}$ is the charging/discharging power of PEV n at time slot t and adopts the following sign convention: when $x_{n,t} > 0$, the PEV n is charging; when $x_{n,t} < 0$, the PEV is discharging; and when $x_{n,t} = 0$, the PEV is idle. Let $\boldsymbol{x} = (\boldsymbol{x_1}^T, \boldsymbol{x_2}^T, \ldots, \boldsymbol{x_N}^T)^T$ represent the charging profile of all PEVs in SCS.

A. System Model

1) Feasible Charging Profile Set: Assume that the initial and terminal energy levels of PEV n are π_n^0 and π_n^T, respectively. Then the required energy of PEV n is $R_n = \pi_n^T - \pi_n^0$. One thus has

$$\sum_{t=1}^{T} x_{n,t} = R_n, \ \forall n \in \mathcal{N}, \tag{1}$$

which indicates that during the entire charging period, the total energy consumption of PEV n should be equal to the required energy such that the terminal energy level is reached at the end of charging without overcharging. Moreover, the energy level of each PEV $n \in \mathcal{N}$ after being charged or discharged at any time cannot exceed its battery capacity, i.e.,

$$\pi_n^{min} \le \pi_n^0 + \sum_{\tau=1}^{t} x_{n,\tau} \le \pi_n^{max}, \ \forall t \in \mathcal{T}, \forall n \in \mathcal{N}, \tag{2}$$

where π_n^{min} and π_n^{max} are the lower and upper battery capacity of PEV n, respectively. The charging/discharging power of each PEV n at any time $t \in \mathcal{T}$ is bounded by

$$-x_n^{max} \le x_{n,t} \le x_n^{max}, \ \forall t \in \mathcal{T}, \forall n \in \mathcal{N}, \tag{3}$$

where x_n^{max} and $-x_n^{max}$ are the rated charging and discharging power of PEV n, respectively.

In addition, for safety, the total charging request of all PEVs at any time cannot exceed the maximum allowable load of SCS, i.e.,

$$0 \le \sum_{n=1}^{N} x_{n,t} \le L_{max}, \ \forall t \in \mathcal{T}, \tag{4}$$

where L_{max} is the maximum allowable load of SCS.

Therefore, for each PEV n, the feasible charging profile set is as follows:

$$\boldsymbol{\mathcal{X}_n} = \{\boldsymbol{x_n} | (1) - (4)\}. \tag{5}$$

Correspondingly, the feasible charging profile set of all PEVs in SCS is $\boldsymbol{\mathcal{X}} = \{(\boldsymbol{x_1}, \boldsymbol{x_2}, \ldots, \boldsymbol{x_N}) | \boldsymbol{x_n} \in \boldsymbol{\mathcal{X}_n}, \forall n \in \mathcal{N}\}$.

2) Electricity Price Model: To coordinate the charging behaviors of PEVs, the following linear price function [17] is introduced

$$p_t = \alpha_t L_t + \beta_t, \ \forall t \in \mathcal{T}, \tag{6}$$

where α_t and β_t are positive price coefficients related to the TOU price and the base price of SCS, respectively[2]; $L_t = \sum_{n=1}^{N} x_{n,t}$ is the total aggregate load of SCS at time slot t. Notice that the price function is increasing, which prevents the SCS from overloading. Specifically, if there is a significant increase in aggregate load of SCS resulting from charging too many PEVs at the same time, the price will rise accordingly to prompt PEVs without urgent tasks to shift their charging requests to low-price periods.

3) Cost Model of SCS: Given the price p_t, we define $C_t(L_t)$ as the energy cost of SCS at time slot t, indicating the fees paid by SCS to a higher-level power supply facility. In general, the cost model must satisfy the following assumption:

Assumption 1: [23] The cost function $C_t(L_t)$ is considered to be non-decreasing with respect to (w.r.t.) the aggregate load L_t at each time slot $t \in \mathcal{T}$. That is, the following property holds:

$$\frac{\partial C_t(L_t)}{\partial L_t} \ge 0, \ \forall t \in \mathcal{T}. \tag{7}$$

A typical cost model that satisfies Assumption 1 can be expressed as a quadratic function [24], [25], i.e.,

$$C_t(L_t) = p_t L_t = \alpha_t L_t^2 + \beta_t L_t, \ \forall t \in \mathcal{T}. \tag{8}$$

The total energy cost of SCS over the entire charging horizon is then written as

$$C_{tol} = \sum_{t=1}^{T} C_t(L_t). \tag{9}$$

In addition, we define f_n as the fees paid by the owner of PEV n at the end of charging, which depends on the electricity price and the total energy consumption of PEV n over the entire charging period. Without loss of generality, the total fees paid by all PEVs should be greater than the total energy cost of SCS. That is to say, it must ensure that the SCS does not lose money or at least makes ends meet,

[2]The base price of a SCS depends largely on the distance to the power plants. Generally, the farther away from the power plants, the higher the base price of SCS.

i.e., $\sum_{n=1}^{N} f_n \geq \sum_{t=1}^{T} C_t(L_t)$. Next, we define a profitability index $\delta := \frac{\sum_{n=1}^{N} f_n}{\sum_{t=1}^{T} C_t(L_t)}$ to measure whether the SCS is profitable. Obviously, if $\delta = 1$, the SCS makes ends meet; if $\delta > 1$, the SCS is profitable. Note that the price charged by SCS to PEVs is fixed, and therefore the fees paid by the owners of PEVs is proportional to their total energy consumption over the entire charging period, i.e.,

$$\frac{f_n}{f_m} = \frac{\sum_{t=1}^{T} x_{n,t}}{\sum_{t=1}^{T} x_{m,t}}, \ \forall n, m \in \mathcal{N}. \tag{10}$$

Sum up both sides of equality (10) over all PEVs to yield

$$f_n = \frac{\sum_{t=1}^{T} x_{n,t}}{\sum_{m\in\mathcal{N}} \sum_{t=1}^{T} x_{m,t}} \sum_{m\in\mathcal{N}} f_m. \tag{11}$$

Combining the definition of δ and (11), one has

$$\begin{aligned} f_n &= \frac{\delta \sum_{t=1}^{T} x_{n,t}}{\sum_{m\in\mathcal{N}} \sum_{t=1}^{T} x_{m,t}} \sum_{t=1}^{T} C_t(L_t) = \gamma_n \sum_{t=1}^{T} (\alpha_t L_t^2 + \beta_t L_t) \\ &= \gamma_n \sum_{t=1}^{T} \big[\alpha_t (\sum_{n=1}^{N} x_{n,t})^2 + \beta_t \sum_{n=1}^{N} x_{n,t}\big], \end{aligned} \tag{12}$$

where $\gamma_n = \delta \xi_n$ with $\xi_n = \frac{\sum_{t=1}^{T} x_{n,t}}{\sum_{m\in\mathcal{N}} \sum_{t=1}^{T} x_{m,t}}$ as the proportion of the total energy consumption of PEV n in the total aggregate load of SCS.

B. Problem formulation

As previously mentioned, the charging coordination is to collectively determine the optimal charging profile of all PEVs so as to minimize the total energy cost of SCS while satisfying the charging needs of PEVs and the constraints of SCS. The problem can be formulated as follows:

$$\begin{cases} \min\limits_{\boldsymbol{x}\in\boldsymbol{\mathcal{X}}} \ C_{tol} = \sum\limits_{t=1}^{T} C_t(L_t), \\ \text{s. t. } (5), \ \forall n \in \mathcal{N}. \end{cases} \tag{13}$$

Since the feasible charging profile set $\boldsymbol{\mathcal{X}_n}$ is bounded by a finite set of linear constraints (1)-(4), the set $\boldsymbol{\mathcal{X}_n}$ is nonempty, compact, and convex. Moreover, the cost function $C_t(\cdot)$ with the form (8) is strictly convex. Thus, the optimization problem (13) is convex and has a unique optimal solution [26].

III. Non-Cooperative PEV Charging Game

This section first constructs a non-cooperative game framework for PEVs charging, and then discusses the existence and optimality of the NE solution.

A. Game Model

In SCS, each PEV tries to select an optimal charging strategy from its strategy set to minimize its payment to SCS. Therefore, a *non-cooperative PEV charging game* $\mathcal{G} = \{\mathcal{N}, \{\boldsymbol{\mathcal{X}_n}\}_{n\in\mathcal{N}}, \{f_n\}_{n\in\mathcal{N}}\}$ is formulated, in which each component is described as follows:

- *Players*: The PEVs in set $\mathcal{N}$;
- *Strategy set*: $\boldsymbol{\mathcal{X}_n} \subseteq \mathbb{R}^T$ for each $n \in \mathcal{N}$, is nonempty, compact, and convex;
- *Cost function*: $f_n(\boldsymbol{x_n}, \boldsymbol{x_{-n}})$ for each $n \in \mathcal{N}$ shown as

$$f_n(\boldsymbol{x_n}, \boldsymbol{x_{-n}}) = \gamma_n \sum_{t=1}^{T} \big[\alpha_t (\sum_{n=1}^{N} x_{n,t})^2 + \beta_t \sum_{n=1}^{N} x_{n,t}\big], \tag{14}$$

where $\boldsymbol{x_{-n}} = (\boldsymbol{x_1}, \ldots, \boldsymbol{x_{n-1}}, \boldsymbol{x_{n+1}} \ldots, \boldsymbol{x_N})$ represents the strategies of all players except that of player n. In this regard, the vector $\boldsymbol{x}$ is usually written as $\boldsymbol{x} = (\boldsymbol{x_n}, \boldsymbol{x_{-n}})$ to stress the player n's strategy in game theory [15]. It is assumed that all players are rational in the sense of minimizing their own payments to SCS. Moreover, it can be observed from (14) that the individual cost of each palyer depends on both its own strategy and all other PEVs' strategies.

Definition 1: Consider the *non-cooperative PEV charging game* $\mathcal{G} = \{\mathcal{N}, \{\boldsymbol{\mathcal{X}_n}\}_{n\in\mathcal{N}}, \{f_n\}_{n\in\mathcal{N}}\}$ with $\boldsymbol{\mathcal{X}_n}$ and f_n given by (5) and (14), respectively. A vector $\boldsymbol{x}^* = (\boldsymbol{x_n^*}, \boldsymbol{x_{-n}^*}) \in \boldsymbol{\mathcal{X}}$ is a NE of $\mathcal{G}$ if and only if the following inequality holds:

$$f_n(\boldsymbol{x_n^*}, \boldsymbol{x_{-n}^*}) \leq f_n(\boldsymbol{x_n}, \boldsymbol{x_{-n}^*}), \forall (\boldsymbol{x_n}, \boldsymbol{x_{-n}^*}) \in \boldsymbol{\mathcal{X}}, \forall n \in \mathcal{N}. \tag{15}$$

That is, no player can unilaterally deviate from NE strategy to reduce its payment.

Note that in game theory, a solution of a non-cooperative game is a NE which characterizes how players play the game.

Remark 1: Some existing works have adopted the dominant strategy equilibrium (DSE), a strategy combination composed of the dominant strategies of all participants, to characterize the player's self-interested behavior [27]. At the DSE, each player always follows the dominant strategy regardless of other players' strategies. However, in problem (13), the feasible set of each player depends on other players' strategies according to (1)-(4). Therefore, under the V2V mechanism considered in the current work that allows the strategic interactions among players, the NE is more suitable than the DSE.

B. Existence and Optimality of NE

Next, we proceed to seek a NE of the game $\mathcal{G}$. Since the NE may not exist in non-cooperative games, it is necessary to discuss the existence of NE. The next theorem shows the existence of NE for our formulated game $\mathcal{G}$.

Theorem 1: Consider the *non-cooperative PEV charging game* $\mathcal{G} = \{\mathcal{N}, \{\boldsymbol{\mathcal{X}_n}\}_{n\in\mathcal{N}}, \{f_n\}_{n\in\mathcal{N}}\}$ with $\boldsymbol{\mathcal{X}_n}$ and f_n given by (5) and (14), respectively. Then, the NE of game $\mathcal{G}$ always exists.

Proof: The Hessian matrix of cost function $f_n(\boldsymbol{x_n}, \boldsymbol{x_{-n}})$ w.r.t the charging strategy $\boldsymbol{x_n}$ is give by $\frac{\partial^2 f_n(\boldsymbol{x_n}, \boldsymbol{x_{-n}})}{\partial \boldsymbol{x_n}^2} = \text{diag}\{2\gamma_n\alpha_1, 2\gamma_n\alpha_2, \cdots, 2\gamma_n\alpha_T\}$, where $\gamma_n = \delta\xi_n \geq 0$ and $\alpha_t > 0$ for each $t \in \mathcal{T}$. Then the Hessian matrix is positive semidefinite since it is diagonal with nonnegative diagonal elements. The cost function $f_n(\boldsymbol{x_n}, \boldsymbol{x_{-n}})$ is thereby convex w.r.t. $\boldsymbol{x_n}$. Moreover, it is noted that the strategy set $\boldsymbol{\mathcal{X}_n}$ bounded by a finite set of linear constraints is nonempty, compact, and convex. Therefore, by Theorem 4.1 in [28], the NE of game $\mathcal{G}$ always exists. ■

This article has been accepted for publication in a future issue of this journal, but has not been fully edited. Content may change prior to final publication. Citation information: DOI 10.1109/TSG.2020.3020466, IEEE Transactions on Smart Grid

In what follows, we further discuss the optimality of NE for game $\mathcal{G}$ (see Theorem 2 below).

Theorem 2: The unique NE of *non-cooperative PEV charging game* $\mathcal{G}$ is exactly the optimal solution to energy cost minimization problem (13).

Proof: Denote $\boldsymbol{x}^* = (\boldsymbol{x}^*_{\boldsymbol{n}}, \boldsymbol{x}^*_{-\boldsymbol{n}}) \in \boldsymbol{\mathcal{X}}$ as a NE of $\mathcal{G}$, then by (15), one has

$$\begin{aligned}&\gamma_n \sum_{t=1}^{T} \big[\alpha_t(\sum_{n\in\mathcal{N}} x^*_{n,t})^2 + \beta_t \sum_{n\in\mathcal{N}} x^*_{n,t}\big] \\ \leq&\gamma_n \sum_{t=1}^{T} \big[\alpha_t(x_{n,t} + \sum_{m\in\mathcal{N},m\neq n} x^*_{m,t})^2 + \beta_t(x_{n,t} + \sum_{m\in\mathcal{N},m\neq n} x^*_{m,t})\big].\end{aligned} \tag{16}$$

Dividing both sides of (16) by γ_n yields

$$\begin{aligned}C^*_{tol} \leq \sum_{t=1}^{T} \big[&\alpha_t(x_{n,t} + \sum_{m\in\mathcal{N},m\neq n} x^*_{m,t})^2 \\ &+ \beta_t(x_{n,t} + \sum_{m\in\mathcal{N},m\neq n} x^*_{m,t})\big].\end{aligned} \tag{17}$$

Therefore, it can be obtained that the NE of game $\mathcal{G}$ is the optimal solution to problem (13). In addition, we have learned that the optimization problem (13) has a unique optimal solution. It is then concluded that the NE of game $\mathcal{G}$ is unique and is exactly the optimal solution to energy cost minimization problem (13). ■

IV. Distributed GNE-Seeking Algorithm

In this section, we propose a GNE-seeking algorithm based on the Newton fixed-point method. And a distributed fast-ADMM framework is employed to determine the best response of PEVs. Since that both strategy set $\boldsymbol{\mathcal{X}}_{\boldsymbol{n}}$ and cost function f_n of PEV n depend on the strategies of all other PEVs, the formulated game $\mathcal{G}$ can be further regarded as a generalized Nash equilibrium problem (GNEP) [28]. Therefore, the previously mentioned NE of game $\mathcal{G}$ corresponds to the generalized Nash equilibrium (GNE), which is a solution of GNEP and also characterizes how players play a game. Unless otherwise stated, hereinafter we replace the NE with GNE.

A. GNE-Seeking Algorithm Based on Newton Fixed-Point Method

We first introduce a ρ-regularized Nikaido-Isoda (NI) function [28]

$$\varphi_\rho(\boldsymbol{x},\boldsymbol{y}) := \sum_{n=1}^{N} \big[f_n(\boldsymbol{x_n},\boldsymbol{x_{-n}}) - f_n(\boldsymbol{y_n},\boldsymbol{x_{-n}}) - \frac{\rho}{2}\|\boldsymbol{x_n}-\boldsymbol{y_n}\|^2\big] \tag{18}$$

with a suitable regularization parameter $\rho > 0$, which represents the cost reduction of PEV n when he changes his charging strategy $\boldsymbol{x_n}$ to another feasible strategy $\boldsymbol{y_n} \in \boldsymbol{\mathcal{X}_n}$ while all other PEVs still adopt the original strategies $\boldsymbol{x_{-n}}$. That is to say, the ρ-regularized NI function quantifies how much the individual PEV benefits when he unilaterally changes his strategy while leaving the strategies of other PEVs unchanged.

Based on the ρ-regularized NI function, we further define

$$V_\rho(\boldsymbol{x}) := \max_{\boldsymbol{y}\in\boldsymbol{\mathcal{X}}} \ \varphi_\rho(\boldsymbol{x},\boldsymbol{y}). \tag{19}$$

Since $\varphi_\rho(\boldsymbol{x},\boldsymbol{y})$ is strongly concave w.r.t $\boldsymbol{y}$ for any $\boldsymbol{x} \in \boldsymbol{\mathcal{X}}$, there exists a unique maximizer $\boldsymbol{y}_\rho(\boldsymbol{x})$ such that

$$\begin{aligned}\boldsymbol{y}_\rho(\boldsymbol{x}) &= \arg\max_{\boldsymbol{y}\in\boldsymbol{\mathcal{X}}} \ \varphi_\rho(\boldsymbol{x},\boldsymbol{y}) \\ &= \arg\min_{\boldsymbol{y}\in\boldsymbol{\mathcal{X}}} \ \sum_{n=1}^{N} \big[f_n(\boldsymbol{y_n},\boldsymbol{x_{-n}}) + \frac{\rho}{2}\|\boldsymbol{x_n}-\boldsymbol{y_n}\|^2\big].\end{aligned} \tag{20}$$

According to Theorem 5.4 in [28], one has $V_\rho(\boldsymbol{x}) \geq 0$ for all $\boldsymbol{x} \in \boldsymbol{\mathcal{X}}$ and $\boldsymbol{x}^*$ is a GNE of jointly convex GNEP if and only if $\boldsymbol{x}^* \in \boldsymbol{\mathcal{X}}$ and $V_\rho(\boldsymbol{x}^*) = 0$. With this in mind, one further concludes that $\boldsymbol{x}^*$ is a fixed point of the following mapping system (see Theorem 5.5 in [28]):

$$M(\boldsymbol{x}^*) := \boldsymbol{y}_\rho(\boldsymbol{x}^*) - \boldsymbol{x}^* = 0. \tag{21}$$

Next, we employ the Newton method to solve the mapping system (21) [18], [29], [30], in which $\boldsymbol{x}$ is updated by

$$\boldsymbol{x}^{k+1} = \boldsymbol{x}^k + \Delta\boldsymbol{x}^k, \tag{22}$$

where $\Delta\boldsymbol{x}^k$ is the Newton direction at k-th iteration which is computed by solving the following linear system

$$H^k\Delta\boldsymbol{x}^k = -M(\boldsymbol{x}^k), \tag{23}$$

where H^k is an entry of the computable generalized Jacobian of M at $\boldsymbol{x}^k$, i.e.,

$$H^k \in \partial M(\boldsymbol{x}^k) = \{\nabla\boldsymbol{y}_\rho(\boldsymbol{x}^k)^T - I\}, \tag{24}$$

where $I \in R^{NT\times NT}$ is an identity matrix. The nonsingularity of the generalized Jacobian can be easily guaranteed by weak conditions (see Lemma 4.2 in [29]). Then, the details of the distributed GNE-seeking algorithm based on Newton fixed-point method is summarized in Algorithm 1.

Algorithm 1 GNE-Seeking Algorithm Based on Newton Fixed-Point Method

Output: GNE $\boldsymbol{x}^*$ of *Game* $\mathcal{G}$
Initialize: Set $\rho, \epsilon_1 > 0, \boldsymbol{x}^0_n \in \boldsymbol{\mathcal{X}}_n$ for $\forall n \in \mathcal{N}, k = 0$;
Repeat
  Step 1: Compute $\boldsymbol{y}^k$ by solving (20), i.e.,
  $\boldsymbol{y}^k = \arg\min_{\boldsymbol{y}\in\boldsymbol{\mathcal{X}}} \sum_{n=1}^{N} \big[f_n(\boldsymbol{y_n},\boldsymbol{x}^{\boldsymbol{k}}_{\boldsymbol{-n}}) + \frac{\rho}{2}\|\boldsymbol{x}^{\boldsymbol{k}}_{\boldsymbol{n}} - \boldsymbol{y_n}\|^2\big]$;
  Step 2: Compute generalized Jacobian H^k by (24);
  Step 3: Solve the linear system (23) to calculate the Newton direction $\Delta\boldsymbol{x}^k$, i.e.,
  $\Delta\boldsymbol{x}^k = -(H^k)^{-1}M(\boldsymbol{x}^k) = -(H^k)^{-1}(\boldsymbol{y}^k - \boldsymbol{x}^k)$;
  Step 4: Update $\boldsymbol{x}^k$ by $\boldsymbol{x}^{k+1} = \boldsymbol{x}^k + \Delta\boldsymbol{x}^k$;
  Step 5: Check the stopping criterion:
    if $\|\boldsymbol{y}^k - \boldsymbol{x}^k\| \leq \epsilon_1$
      break;
    end if
  Step 6: $k \leftarrow k+1$;
End
Return $\boldsymbol{x}^k$.

This article has been accepted for publication in a future issue of this journal, but has not been fully edited. Content may change prior to final publication. Citation information: DOI 10.1109/TSG.2020.3020466, IEEE Transactions on Smart Grid

Remark 2: Note that in Algorithm 1, the stopping criterion is $\|\boldsymbol{y}^k - \boldsymbol{x}^k\| \le \epsilon_1$ instead of the commonly used $\|\boldsymbol{x}^{k+1} - \boldsymbol{x}^k\| \le \epsilon_1$. The main reason is that Algorithm 1 aims to seek the GNE of game $\mathcal{G}$, so we have to guarantee that we get the GNE at the end of the algorithm. To this end, the first step of Algorithm 1 is to seek the PEVs' best response, which corresponds to the optimal strategy of each PEV given all other PEVs' strategies. Then by the Newton fixed-point method, we update $\boldsymbol{x}$ to find the GNE. Since all players obtain the optimal strategies at the best response, in this sense, the best response at the end of the algorithm is essentially equivalent to the GNE. Therefore, in each iteration, we can check the difference of the best response and GNE to determine whether the algorithm is terminated.

B. Fast-ADMM Framework for PEVs' Best Response

Note that in each iteration of Algorithm 1, we need to solve a subproblem (20) to determine the best response of PEVs under a given strategy $\boldsymbol{x}$. Although some traditional convex programming techniques such as interior point method (IPM) [26] can solve such optimization subproblem, it is undesirable when considering the system scalability and reliability. As a result, we next employ the fast-ADMM framework [31] which can be achieved in a distributed manner, ensuring scalability and reliability of the system.

By introducing an auxiliary vector $\boldsymbol{z}$ (a common trick in ADMM), the subproblem (20) can be reformulated as

$$\begin{cases} \min \sum_{n=1}^{N} \left[f_n(\boldsymbol{y}_n, \boldsymbol{x}_{-n}^k) + \frac{\rho}{2}\|\boldsymbol{x}_n^k - \boldsymbol{y}_n\|^2 \right] + I_1(\boldsymbol{y}) + I_2(\boldsymbol{z}), \\ \text{s.t. } \boldsymbol{y} = \boldsymbol{z}, \end{cases} \tag{25}$$

where $I_1(\boldsymbol{y})$ and $I_2(\boldsymbol{z})$ are indicator functions. $I_1(\boldsymbol{y}) = 0$ if $\boldsymbol{y} \in S_1$ and $I_1(\boldsymbol{y}) = \infty$ otherwise with set $S_1 = \{\boldsymbol{y} | \pi_n^{min} \le \pi_n^0 + \sum_{\tau=1}^{t} y_{n,\tau} \le \pi_n^{max}, \forall t \in \mathcal{T}, \forall n \in \mathcal{N}; -y_n^{max} \le y_{n,t} \le y_n^{max}, \forall t \in \mathcal{T}, \forall n \in \mathcal{N}; 0 \le \sum_{n=1}^{N} y_{n,t} \le L_{max}, \forall t \in \mathcal{T}\}$. $I_2(\boldsymbol{z}) = 0$ if $\boldsymbol{z} \in S_2$ and $I_2(\boldsymbol{z}) = \infty$ otherwise with set $S_2 = \{\boldsymbol{z} | \sum_{t=1}^{T} z_{n,t} = R_n, \forall n \in \mathcal{N}\}$. The augmented Lagrangian of (25) is

$$\begin{aligned} L_\zeta(\boldsymbol{y}, \boldsymbol{z}, \boldsymbol{\lambda}) = &\sum_{n=1}^{N} \left[f_n(\boldsymbol{y}_n, \boldsymbol{x}_{-n}^k) + \frac{\rho}{2}\|\boldsymbol{x}_n^k - \boldsymbol{y}_n\|^2 \right] + I_1(\boldsymbol{y}) \\ &+ I_2(\boldsymbol{z}) + \boldsymbol{\lambda}^T(\boldsymbol{z} - \boldsymbol{y}) + \frac{\zeta}{2}\|\boldsymbol{z} - \boldsymbol{y}\|^2, \end{aligned} \tag{26}$$

where $\boldsymbol{\lambda} \in \mathbb{R}^{TN}$ is the Lagrange multiplier vector and ζ is the augmented Lagrange multiplier.

Motivated by the work in [25] and [31], a fast-ADMM framework composed by the standard ADMM and a predictor-corrector acceleration step is employed to determine the best response of PEVs in a distributed manner. The details are shown in Algorithm 2.

C. Convergence Analysis

Next, we provide the convergence analysis on Algorithms 1 and 2. The results are shown in the following theorems.

Algorithm 2 Best Response of PEVs under fast-ADMM Framework

Output: Best response $\boldsymbol{y}^k$ of all PEVs
Initialize: Set $\boldsymbol{z}^0 = \hat{\boldsymbol{z}}^1 \in \mathbb{R}^{TN}$, $\boldsymbol{\lambda}^0 = \hat{\boldsymbol{\lambda}}^1 \in \mathbb{R}^{TN}$, $\epsilon_2 > 0$, $\zeta > 0$, $\eta^1 = 1$, and a given charging strategy $\boldsymbol{x}$;
Repeat
  for $\nu = 1, 2, \cdots$ **do**
    $\boldsymbol{y}$-update: $\boldsymbol{y}^\nu = \arg\min_{\boldsymbol{y} \in S_1} L_\zeta(\boldsymbol{y}, \hat{\boldsymbol{z}}^\nu, \hat{\boldsymbol{\lambda}}^\nu)$;
    $\boldsymbol{z}$-update: $\boldsymbol{z}^\nu = \arg\min_{\boldsymbol{z} \in S_2} L_\zeta(\boldsymbol{y}^\nu, \boldsymbol{z}, \hat{\boldsymbol{\lambda}}^\nu)$;
    $\boldsymbol{\lambda}$-update: $\boldsymbol{\lambda}^\nu = \hat{\boldsymbol{\lambda}}^\nu + \zeta(\boldsymbol{z}^\nu - \boldsymbol{y}^\nu)$;
    Predictor-corrector step:
      $\eta^{\nu+1} = \frac{1+\sqrt{1+4(\eta^\nu)^2}}{2}$;
      $\hat{\boldsymbol{z}}^{\nu+1} = \boldsymbol{z}^\nu + \frac{\eta^\nu - 1}{\eta^{\nu+1}}(\boldsymbol{z}^\nu - \boldsymbol{z}^{\nu-1})$;
      $\hat{\boldsymbol{\lambda}}^{\nu+1} = \boldsymbol{\lambda}^\nu + \frac{\eta^\nu - 1}{\eta^{\nu+1}}(\boldsymbol{\lambda}^\nu - \boldsymbol{\lambda}^{\nu-1})$;
  Until $\|\boldsymbol{\lambda}^\nu - \boldsymbol{\lambda}^{\nu-1}\| \le \epsilon_2$
End
Return $\boldsymbol{y}^\nu$.

Theorem 3: Consider the *non-cooperative PEV charging game* $\mathcal{G} = \{\mathcal{N}, \{\boldsymbol{\mathcal{X}}_{\boldsymbol{n}}\}_{n\in\mathcal{N}}, \{f_n\}_{n\in\mathcal{N}}\}$ with $\boldsymbol{\mathcal{X}}_{\boldsymbol{n}}$ and f_n given by (5) and (14), respectively. Then, the sequence $\{\boldsymbol{x}^k\}$ generated by Algorithm 1 converges Q-quadratically to a GNE.

Proof: We first notice that since the strategy set $\boldsymbol{\mathcal{X}}$ is composed by a finite set of linear constraints, the constant rank constraint qualification (CRCQ)[3] of Assumption 3.1 in [29] is satisfied. Next, by the proof of Theorem 1, it can be seen that for each $n \in \mathcal{N}$, the Hessian matrix $\frac{\partial^2 f_n(\boldsymbol{x_n}, \boldsymbol{x_{-n}})}{\partial \boldsymbol{x_n}^2}$ w.r.t the charging strategy $\boldsymbol{x_n}$ is positive semidefinite. Thus, the Assumption 4.1 in [29] is also satisfied. Then, the nonsingularity of the generalized Jacobian $\partial M(\boldsymbol{x}^k), \boldsymbol{x}^k \in \boldsymbol{\mathcal{X}}$ directly holds due to Lemma 4.2 in [29]. Let $\boldsymbol{x}^*$ be a GNE of game $\mathcal{G}$, then $\{\nabla \boldsymbol{y}_\rho(\boldsymbol{x}^*)^T - I\}$ is thereby nonsingular, which also implies that $\boldsymbol{x}^*$ is a quasi-regular solution[4] to system (21). Therefore, it can be readily obtained from Theorem 2 in [30] that the Newton-type method is well defined and the sequence $\{\boldsymbol{x}^k\}$ generated by Algorithm 1 converges Q-quadratically to $\boldsymbol{x}^*$. ■

Next, the convergence result for Algorithm 2 is provided.

Theorem 4: The sequence $\{(\boldsymbol{y}^\nu, \boldsymbol{z}^\nu, \boldsymbol{\lambda}^\nu)\}$ generated by Algorithm 2 converges to a KKT point $(\boldsymbol{y}^*, \boldsymbol{z}^*, \boldsymbol{\lambda}^*)$ of problem (25). Moreover, at $(\boldsymbol{y}^*, \boldsymbol{z}^*, \boldsymbol{\lambda}^*)$, the Lagrangian (26) converges to the ϵ_2-optimal solution with the following upper bound:

$$L_\zeta(\boldsymbol{y}^*, \boldsymbol{z}^*, \boldsymbol{\lambda}^*) - L_\zeta(\boldsymbol{y}^{\nu+1}, \boldsymbol{z}^{\nu+1}, \boldsymbol{\lambda}^{\nu+1}) \le \frac{2\|\boldsymbol{\lambda}^0 - \boldsymbol{\lambda}^*\|^2}{\zeta(\nu+2)^2} \tag{27}$$

Proof: Note that the optimal solution to problem (25) must satisfy the KKT conditions which are shown below:

$$\boldsymbol{y}^* = \boldsymbol{z}^*, \tag{28}$$

[3] The constant rank constraint qualification (CRCQ) holds if for each subset of the gradients of the active inequality constraints and the gradients of the equality constraints, the rank at a vicinity of x^* is constant [32].

[4] A point $\boldsymbol{x}$ is a quasi-regular solution to system (21) if all matrices in the generalized Jacobian $\partial M(\boldsymbol{x}^k)$ are nonsingular [30].

$$0 \in \frac{\partial f_n(\boldsymbol{y_n}, \boldsymbol{x^k_{-n}})}{\partial y^*_{n,t}} - \rho(x^k_{n,t} - y^*_{n,t}) + \mathcal{M}_1 - \lambda^*_{n,t} - \zeta(z^*_{n,t} - y^*_{n,t}), \tag{29}$$

$$0 \in \mathcal{M}_2 + \lambda^*_{n,t} + \zeta(z^*_{n,t} - y^*_{n,t}), \tag{30}$$

$$\lambda^*_{n,t} \neq 0, \tag{31}$$

where $\mathcal{M}_1$ and $\mathcal{M}_2$ are subgradient sets of indicator functions $I_1(\boldsymbol{y})$ and $I_2(\boldsymbol{z})$ w.r.t $y^*_{n,t}$ and $z^*_{n,t}$, respectively. While in each iteration of Algorithm 2, the $\boldsymbol{y}$-update and $\boldsymbol{z}$-update always satisfy the conditions (29) and (30), respectively. Moreover, when Algorithm 2 stops, one has $\boldsymbol{\lambda}^\nu \rightarrow \boldsymbol{\lambda}^{\nu-1}$, which implies $\boldsymbol{\lambda}^\nu \rightarrow \hat{\boldsymbol{\lambda}}^\nu$. Then one further obtains condition (28). As for the last condition (31), it is straightforward by $\boldsymbol{\lambda}$-update. Therefore, the sequence $\{(\boldsymbol{y}^\nu, \boldsymbol{z}^\nu, \boldsymbol{\lambda}^\nu)\}$ generated by Algorithm 2 converges to a KKT point of problem (25).

By the Lagrangian (26), one obtains

$$\begin{aligned} &L_\zeta(\boldsymbol{y}^{\nu+1}, \boldsymbol{z}^{\nu+1}, \boldsymbol{\lambda}^{\nu+1}) - L_\zeta(\boldsymbol{y}^\nu, \boldsymbol{z}^\nu, \boldsymbol{\lambda}^\nu) \\ \geq &\frac{1}{2\zeta}\|\boldsymbol{\lambda}^{\nu+1} - \hat{\boldsymbol{\lambda}}^{\nu+1}\|^2 + \frac{1}{\zeta}(\boldsymbol{\lambda}^{\nu+1} - \hat{\boldsymbol{\lambda}}^{\nu+1})^T(\hat{\boldsymbol{\lambda}}^{\nu+1} - \boldsymbol{\lambda}^\nu) \end{aligned} \tag{32}$$

and

$$\begin{aligned} &L_\zeta(\boldsymbol{y}^{\nu+1}, \boldsymbol{z}^{\nu+1}, \boldsymbol{\lambda}^{\nu+1}) - L_\zeta(\boldsymbol{y}^*, \boldsymbol{z}^*, \boldsymbol{\lambda}^*) \\ \geq &\frac{1}{2\zeta}\|\boldsymbol{\lambda}^{\nu+1} - \hat{\boldsymbol{\lambda}}^{\nu+1}\|^2 + \frac{1}{\zeta}(\boldsymbol{\lambda}^{\nu+1} - \hat{\boldsymbol{\lambda}}^{\nu+1})^T(\hat{\boldsymbol{\lambda}}^{\nu+1} - \boldsymbol{\lambda}^*) \end{aligned} \tag{33}$$

Denote $\Delta_\nu = L_\zeta(\boldsymbol{y}^*, \boldsymbol{z}^*, \boldsymbol{\lambda}^*) - L_\zeta(\boldsymbol{y}^\nu, \boldsymbol{z}^\nu, \boldsymbol{\lambda}^\nu)$. Then by combining (32), one gets

$$\begin{aligned} &-\Delta_{\nu+1} + \Delta_\nu \\ \geq &\frac{1}{2\zeta}\|\boldsymbol{\lambda}^{\nu+1} - \hat{\boldsymbol{\lambda}}^{\nu+1}\|^2 + \frac{1}{\zeta}(\boldsymbol{\lambda}^{\nu+1} - \hat{\boldsymbol{\lambda}}^{\nu+1})^T(\hat{\boldsymbol{\lambda}}^{\nu+1} - \boldsymbol{\lambda}^\nu). \end{aligned} \tag{34}$$

Multiply (34) by $(\eta^{\nu+1} - 1)$ and then substitute it into (33) to yield

$$\begin{aligned} &(\eta^\nu)^2\Delta_\nu - (\eta^{\nu+1})^2\Delta_{\nu+1} \\ \geq &\frac{1}{2\zeta}\|\eta^{\nu+1}(\boldsymbol{\lambda}^{\nu+1} - \hat{\boldsymbol{\lambda}}^{\nu+1})\|^2 + \frac{\eta^{\nu+1}}{\zeta}(\boldsymbol{\lambda}^{\nu+1} - \hat{\boldsymbol{\lambda}}^{\nu+1})^T \\ &\big(\eta^{\nu+1}\hat{\boldsymbol{\lambda}}^{\nu+1} - (\eta^{\nu+1} - 1)\boldsymbol{\lambda}^\nu - \boldsymbol{\lambda}^*\big), \end{aligned} \tag{35}$$

where $\eta^{\nu+1} = \frac{1+\sqrt{1+4(\eta^\nu)^2}}{2}$. In view of the fact that the three vectors $\boldsymbol{a}, \boldsymbol{b}, \boldsymbol{c}$ satisfy the following inequality:

$$\|\boldsymbol{b} - \boldsymbol{a}\|^2 + 2\langle \boldsymbol{b} - \boldsymbol{a}, \boldsymbol{a} - \boldsymbol{c}\rangle = \|\boldsymbol{b} - \boldsymbol{c}\|^2 - \|\boldsymbol{a} - \boldsymbol{c}\|^2, \tag{36}$$

then one obtains

$$\begin{aligned} &2\zeta(\eta^\nu)^2\Delta_\nu - 2\zeta(\eta^{\nu+1})^2\Delta_{\nu+1} \\ \geq &\|\eta^{\nu+1}\boldsymbol{\lambda}^{\nu+1} - \big((\eta^{\nu+1} - 1)\boldsymbol{\lambda}^\nu + \boldsymbol{\lambda}^*\big)\|^2 \\ &- \|\eta^{\nu+1}\hat{\boldsymbol{\lambda}}^{\nu+1} - \big((\eta^{\nu+1} - 1)\boldsymbol{\lambda}^\nu + \boldsymbol{\lambda}^*\big)\|^2. \end{aligned} \tag{37}$$

Moreover, denoting $\boldsymbol{\zeta}_\nu = \eta^\nu\boldsymbol{\lambda}^\nu - (\eta^\nu - 1)\boldsymbol{\lambda}^{\nu-1} - \boldsymbol{\lambda}^*$ and reordering (37), one has

$$2\zeta(\eta^{\nu+1})^2\Delta_{\nu+1} + \|\boldsymbol{\zeta}_{\nu+1}\|^2 \leq 2\zeta(\eta^\nu)^2\Delta_\nu + \|\boldsymbol{\zeta}_\nu\|^2. \tag{38}$$

Note that $\eta^\nu \geq \frac{\nu+2}{2}$ and $\eta^1 = 1$. Thus, one further obtains

$$\begin{aligned} \Delta_{\nu+1} &\leq \frac{4\Delta_1}{(\nu+2)^2} + \frac{2\|\zeta_1\|^2}{\zeta(\nu+2)^2} \\ &= \frac{4\zeta\Delta_1 + 2\|\boldsymbol{\lambda}^1 - \boldsymbol{\lambda}^*\|^2}{\zeta(\nu+2)^2}. \end{aligned} \tag{39}$$

By reviewing (33), one has

$$\begin{aligned} -2\zeta\Delta_1 &= 2\zeta\big(L_\zeta(\boldsymbol{y}^1, \boldsymbol{z}^1, \boldsymbol{\lambda}^1) - L_\zeta(\boldsymbol{y}^*, \boldsymbol{z}^*, \boldsymbol{\lambda}^*)\big) \\ &\geq \|\boldsymbol{\lambda}^1 - \hat{\boldsymbol{\lambda}}^1\|^2 + 2(\boldsymbol{\lambda}^1 - \hat{\boldsymbol{\lambda}}^1)^T(\hat{\boldsymbol{\lambda}}^1 - \boldsymbol{\lambda}^*) \\ &= \|\boldsymbol{\lambda}^1 - \boldsymbol{\lambda}^*\|^2 - \|\hat{\boldsymbol{\lambda}}^1 - \boldsymbol{\lambda}^*\|^2. \end{aligned} \tag{40}$$

Substituting (40) into (39), one immediately gets

$$\Delta_{\nu+1} \leq \frac{2\|\hat{\boldsymbol{\lambda}}^1 - \boldsymbol{\lambda}^*\|^2}{\zeta(\nu+2)^2} = \frac{2\|\boldsymbol{\lambda}^0 - \boldsymbol{\lambda}^*\|^2}{\zeta(\nu+2)^2}, \tag{41}$$

which completes the proof. ■

From the proof of Theorem 4, it can be seen that the fast-ADMM achieves the convergence rate $\mathcal{O}(1/\nu^2)$ while the standard ADMM has a convergence rate $\mathcal{O}(1/\nu)$ [33]. Therefore, at each iteration, the fast-ADMM framework used in this work can determine the PEVs' best response in a more efficient way. In addition, since that the fast-ADMM is essentially a combination of the standard ADMM and a predictive correction step, it does not introduce any complexity. In other words, the complexity of the fast-ADMM algorithm is the same as that of the standard one, which is still linear, i.e., $\mathcal{O}(\mathcal{N})$.

V. Simulation Results

This section presents the simulation results to verify the performance of the proposed distributed GNE-seeking algorithm. For ease of illustration, we first consider a SCS with 10 PEVs in a residential area [18]. Particularly, the effectiveness of Algorithm 2 based on the fast-ADMM framework for PEVs' best response is also verified by comparing with [18] and [33]. Then a large-scale SCS with 150 PEVs in a commercial area is further taken into account to verify the scalability of the proposed algorithm.

A. *Case study 1: SCS with* 10 *PEVs*

In this scenario, 10 heterogeneous PEVs arrive at a residential SCS according to the owners' preferences and needs. The PEVs' parameters, arriving time (AT), and departure time (DT) are listed in Table I. Note that the terminal energy level of PEVs is generally not equal to the maximum capacity of battery to avoid the potential damage to battery. The maximum allowable load of SCS is 50 kWh. The price coefficients are $\alpha_t = 0.2$ \$/kWh at off-peak hours (i.e., from 7:00 to 17:00), $\alpha_t = 0.3$ \$/kWh at peak hours (i.e., from 18:00 to 6:00 of the next day), and $\beta_t = 0.8$ \$/kWh. Note that we consider here the case of $\delta = 1$. Then, the charging strategies without charging coordination are shown in Fig. 3(a). It can be observed from Fig. 3(b) that the peak demand appears from 17:00 to 20:00 and the aggregate load during this period violates the maximum load limit of SCS. The total energy cost

TABLE I. Parameter settings of PEVs

Parameter / PEV	π_n^0	π_n^T	π_n^{min}	π_n^{max}	x_n^{max}	AT	DT
1	7.5	67.5	5	75	15	17:00	22:00
2	6	72	5	80	15	18:00	23:00
3	7	67.5	5	75	10	19:00	6:00
4	5.6	63	5	70	8	17:00	7:00
5	6.7	58.5	5	65	8	18:00	8:00
6	7.5	67.5	5	75	8	12:00	18:00
7	8.1	58.5	5	65	8	11:00	23:00
8	9	72	5	80	10	12:00	6:00
9	7.2	63	5	70	8	13:00	7:00
10	7.5	67.5	5	75	15	14:00	20:00

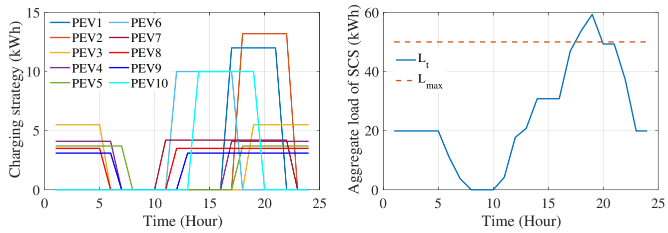

(a) (b)

Fig. 3. (a) Charging strategies without charging coordination. (b) Aggregate load of SCS without charging coordination.

of SCS is \$6298.702. Next, we use the proposed distributed algorithm to coordinate the charging behavior of PEVs, and the results are shown below.

1) Fast ADMM Framework-Based Best Response: To better illustrate the performance of PEVs' best response under the fast-ADMM framework, we take an accelerated gradient algorithm (AGA) proposed in [18] and the standard ADMM algorithm [33] for comparison. In the standard ADMM, let $\rho = 0.1$, $\zeta = 0.01$, and $\epsilon_2 = 0.01$. Figure 4 shows the comparison results. It can be observed that the fast-ADMM

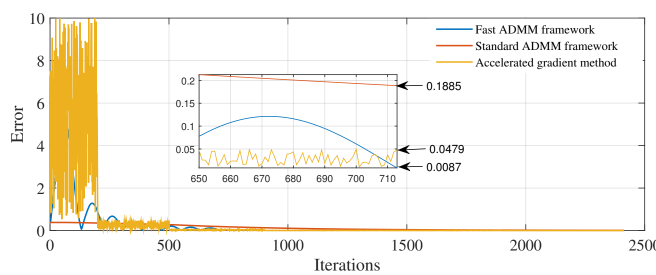

Fig. 4. Convergence performances of three compared algorithms for PEVs' best response.

algorithm converges with an error accuracy of 10^{-2} at 713th iteration while the error accuracy achieved by the standard ADMM framework and the AGA are 0.1885 and 0.0479, respectively. In view of such, it can be concluded that the fast-ADMM framework is superior to the standard one and AGA in terms of the convergence rate.

2) Coordinated Charging Results: Based on the PEVs' best response under the fast-ADMM framework, we further provide the coordinated charging strategies and aggregate load, which are presented in Fig. 5. It can be found from Fig. 5(a) that there are three PEVs discharging at 19:00. As a result, the total aggregate load in Fig. 5(b) does not exceed

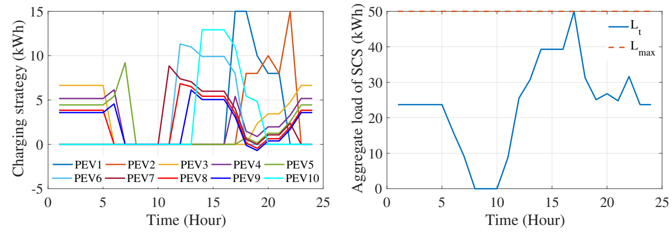

(a) (b)

Fig. 5. (a) Charging strategies with charging coordination. (b) Aggregate load of SCS with charging coordination.

the load limit of SCS. And the total energy cost of SCS is largely reduced from \$6298.702 to \$4670.042 as opposed to the uncoordinated charging. Additionally, as shown in Fig. 6, we provide the iterative process of 10 PEVs at a single time slot, i.e., 19:00, to further illustrate the effectiveness of the proposed algorithm. It can be readily seen that all PEVs

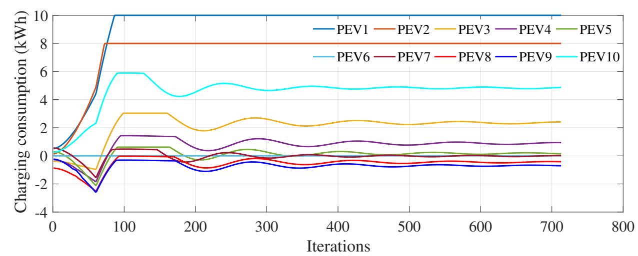

Fig. 6. Charging trajectories of 10 PEVs at 19:00.

converge to their optimal charging strategies. Therefore, the proposed GNE-seeking algorithm under the non-cooperative framework can effectively solve the charging problem in SCS.

B. Case Study 2: Large-Scale SCS with 150 PEVs

To further verify the scalability of the proposed algorithm, we next consider a large-scale SCS located in a commercial area with 150 PEVs charging at daytime, i.e., from 7:00 to 18:00. The load limit of SCS is assumed to be 900 kWh. This scenario considers the case of $\delta = 1.5$ to guarantee the SCS is profitable. The initial charging strategies are depicted in Fig. 7, which shows that in the absence of charging coordination, all PEVs expect to charge as much as possible when connected to SCS, resulting in the overload between 7:30 and 9:30. The total energy cost of SCS is $\$2.425 \times 10^6$.

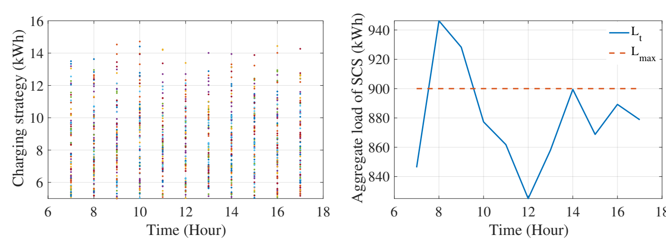

(a) (b)

Fig. 7. (a) Charging strategies without charging coordination. (b) Aggregate load of SCS without charging coordination.

This article has been accepted for publication in a future issue of this journal, but has not been fully edited. Content may change prior to final publication. Citation information: DOI 10.1109/TSG.2020.3020466, IEEE Transactions on Smart Grid

Then, we employ the proposed GNE-seeking algorithm and the coordinated charging strategies are given in Fig. 8. By

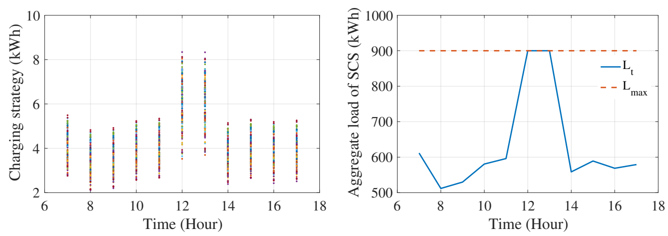

(a) (b)

Fig. 8. (a) Charging strategies with charging coordination. (b) Aggregate load of SCS with charging coordination.

comparing Fig. 7(a) and Fig. 8(a), it can be found that the charging is more dispersed under the coordination. Moreover, Fig. 8(b) shows that there is no violations of load limit with charging coordination, which effectively guarantees the operational security of SCS. Also note that the proposed charging coordination scheme can achieve the peak shaving and valley filling. Additionally, the total energy cost is reduced to $\$1.253 \times 10^6$. Therefore, if the charging strategies of all PEVs depend on the proposed charging coordination scheme, the SCS will operate normally and reduce the cost effectively.

Finally, the computational time of the proposed solution approach for different case studies are presented in TABLE II. It can be readily seen that the proposed algorithm takes 125.05s and 1875.75s to obtain the optimal charging strategies (i.e., GNE of the game $\mathcal{G}$) in a SCS with 10 PEVs and 150PEVs, respectively. Thus, the computational time does not increase dramatically with the increase in the problem size. Therefore, the proposed GNE-seeking algorithm under the non-cooperative framework can effectively solve the charging problem in SCS. In addition, note that the solving time of the internal fast-ADMM for PEVs' best response only accounts for a small fraction of the total computational time, which also indicates the superiority of the fast-ADMM framework.

TABLE II. The computational time for two case studies

	Case study 1		Case study 2	
	Fast-ADMM	GNE-seeking	Fast-ADMM	GNE-seeking
Time/s	49.54	125.05	740.18	1875.75

VI. Conclusion

In this paper, we have formulated a non-cooperative game to investigate the charging problem for PEVs in a SCS, in which the strategic interactions among PEVs are considered. It shows that the GNE of the formulated non-cooperative game exists and is unique. To seek the GNE, we propose a distributed algorithm based on the Newton fixed-point method, in which a fast-ADMM framework is employed to determine the PEVs' best response. Simulation results are provided to illustrate the effectiveness of the proposed algorithm. Notice that since this work mainly focuses on the energy cost minimization on SCS side and the fees paid by the PEVs are closely linked to the SCS's energy cost, the cost function under the formulated non-cooperative game is modeled as the PEVs' payments to SCS. If one takes account of the battery degradation cost of PEVs caused by the charging/discharging, compensation to the PEV owners may be needed to motivate their participation, which will serve as a part of future work.

References

[1] W. Su, H. Eichi, W. Zeng, and M. Chow, "A survey on the electrification of transportation in a smart grid environment," *IEEE Trans. Ind. Informat.*, vol. 8, no. 1, pp. 1-10, Feb. 2012.
[2] S. Rajakaruna, F. Shahnia, and A. Ghosh, *Plug in electric vehicles in smart grids*. Springer, 2016.
[3] Y. Li, C. Davis, Z. Lukszo, and M. Weijnen, "Electric vehicle charging in China' s power system: Energy, economic and environmental trade-offs and policy implications," *Appl. Energy*, vol. 173, pp. 535-554, 2016.
[4] T. Shekari, S. Golshannavaz, and F. Aminifar, "Techno-economic collaboration of PEV fleets in energy management of microgrids," *IEEE Trans. Power Syst.*, vol. 32, no. 5, pp. 3833-3841, Sep. 2017.
[5] N. Rahbari-Asr and M. Chow, "Cooperative distributed demand management for community charging of PHEV/PEVs based on KKT conditions and consensus networks," *IEEE Trans. Ind. Informat.*, vol. 10, no. 3, pp. 1907-1916, Aug. 2014.
[6] P. You, Z. Yang, M. Chow, and Y. Sun, "Optimal cooperative charging strategy for a smart charging station of electric vehicles," *IEEE Trans. Power Syst.*, vol. 31, no. 4, pp. 2946-2956, Jul. 2016.
[7] K. M. Tan, V. K. Ramachandaramurthy, and J. Y. Yong, "Integration of electric vehicles in smart grid: A review on vehicle to grid technologies and optimization techniques," *Renew. Sustain. Energy Rev.*, vol. 53, pp. 720-732, 2016.
[8] H. Shin and R. Baldick, "Plug-in electric vehicle to home V2H operation under a grid outage," *IEEE Trans. Smart Grid*, vol. 8, no. 4, pp. 2032-2041, Jul. 2017.
[9] D. T. Nguyen and L. B. Le, "Joint optimization of electric vehicle and home energy scheduling considering user comfort preference," *IEEE Trans. Smart Grid*, vol. 5, no. 1, pp. 188-199, Jan. 2014.
[10] M. L. Tuballa and M. L. Abundo, "A review of the development of smart grid technologies," *Renew. Sustain. Energy Rev.*, vol. 59, pp. 710-725, 2016.
[11] P. Goli and W. Shireen, "PV powered smart charging station for PHEVs," *Renewable Energy*, vol. 66, pp. 280-287, Jun. 2014.
[12] Y. Cao, S. Tang, C. Li, P. Zhang, Y. Tan, Z. Zhang, and J. Li, "An optimized EV charging model considering TOU price and SOC curve," *IEEE Trans. Smart Grid*, vol. 3, no. 1, pp. 388-393, Mar. 2012.
[13] L. Gan, U. Topcu, and S. H. Low, "Optimal decentralized protocol for electric vehicle charging," *IEEE Trans. Power Syst.*, vol. 28, no. 2, pp. 940-951, May. 2013.
[14] E. Sortomme and M. A. El-Sharkawi, "Optimal charging strategies for unidirectional vehicle-to-grid," *IEEE Trans. Smart Grid*, vol. 2, no. 1, pp. 131-138, Mar. 2011.
[15] R. B. Myerson, *Game theory*. Harvard university press, 2013.
[16] W. Tushar, W. Saad, H. V. Poor, and D. B. Smith, "Economics of electric vehicle charging: A game theoretic approach," *IEEE Trans. Smart Grid*, vol. 3, no. 4, pp. 1767-1778, Dec. 2012.
[17] X. Yang, G. Wang, H. He, J. Lu, and Y. Zhang, "Automated demand response framework in ELNs: Decentralized scheduling and smart contract," *IEEE Trans. Syst., Man, Cybern.*, Syst., vol. 50, no. 1, pp. 58-72, Jan. 2020.
[18] J. Li, C. Li, Y. Xu, Z. Y. Dong, K. P. Wong, and T. Huang, "Noncooperative game-based distributed charging control for plug-in electric vehicles in distribution networks," *IEEE Trans. Ind. Informat.*, vol. 14, no. 1, pp. 301-310, Jan. 2018.
[19] Z. Yang, T. Guo, P. You, Y. Hou, and S. J. Qin, "Distributed approach for temporal-spatial charging coordination of plug-in electric taxi fleet," *IEEE Trans. Ind. Inform.*, vol. 15, no. 6, pp. 3185-3195, Jun. 2019.
[20] C. Li, C. Liu, K. Deng, X. Yu, and T. Huang, "Data-driven charging strategy of PEVs under transformer aging risk," *IEEE Trans. Control Syst. Technol.*, vol. 26, no. 4, pp. 1386-1399, Jul. 2018.
[21] A. Alsabbagh, H. Yin, and C. Ma, "Distributed electric vehicles charging management with social contribution concept," *IEEE Trans. Ind. Inform.*, vol. 16, no. 5, pp. 3483-3492, May. 2020.
[22] W. Fu, J. Qin, Y. Shi, W. X. Zheng, and Y. Kang, "Resilient consensus of discrete-time complex cyber-physical networks under deception attacks," *IEEE Trans. Ind. Inform.*, vol. 16, no. 7, pp. 4868-4877, Jul. 2020.

[23] A. Mohsenian-Rad, V. W. S. Wong, J. Jatskevich, R. Schober, and A. Leon-Garcia, "Autonomous demand-side management based on gametheoretic energy consumption scheduling for the future smart grid," *IEEE Trans. Smart Grid*, vol. 1, no. 3, pp. 320-331, Dec. 2010.

[24] Z. Li, W. Wu, B. Zhang, H. Sun, and Q. Guo, "Dynamic economic dispatch using lagrangian relaxation with multiplier updates based on a quasi-newton method," *IEEE Trans. Power Syst.*, vol. 28, no. 4, pp. 4516-4527, Nov. 2013.

[25] J. Qin, Y. Wan, X. Yu, F. Li, and C. Li, "Consensus-based distributed coordination between economic dispatch and demand response," *IEEE Trans. Smart Grid*, vol. 10, no. 4, pp. 3709-3719, Jul. 2019.

[26] S. Boyd and L. Vandenberghe, *Convex Optimization*. Cambridge University Press, 2004.

[27] S. Li, W. Zhang, J. Lian, and K. Kalsi, "Market-based coordination of thermostatically controlled loads-part I: A mechanism design formulation," *IEEE Trans. Power Syst.*, vol. 31, no. 2, pp. 1170-1178, Mar. 2016.

[28] F. Facchinei and C. Kanzow, "Generalized Nash equilibrium problems," *Ann. Oper. Res.*, vol. 175, no. 1, pp. 177-211, Mar. 2010.

[29] A. von Heusinger, C. Kanzow, and M. Fukushima, "Newton's method for computing a normalized equilibrium in the generalized Nash game through fixed point formulation," *Math. Program.*, vol. 132, no. 1-2, pp. 99-123, Apr. 2012.

[30] F. Facchinei, A. Fischer, and V. Piccialli, "Generalized Nash equilibrium problems and Newton methods," *Math. Program.*, vol. 117, no. 1-2, pp. 163-194, Mar. 2009.

[31] T. Goldstein, B. O' Donoghue, S. Setzer, and R. Baraniuk, "Fast alternating direction optimization methods," *SIAM J. Imag. Sci.*, vol. 7, no. 3, pp. 1588-1623, 2014.

[32] R. Janin, "Direction derivative of the marginal function in nonlinear programming," *Math. Program. Study*, vol. 21, pp. 127-138, Jan. 1984.

[33] S. Boyd, N. Parikh, E. Chu, B. Peleato, and J. Eckstein, "Distributed optimization and statistical learning via the alternating direction method of multipliers," *Found. Trends Mach. Learn.*, vol. 3, no. 1, pp. 1-122, Jan. 2011.

Yanni Wan (S'19) received the B.E. degree in automation from the Ocean University of China, Qingdao, China, in 2016.

She is currently pursuing the Ph.D. degree in control science and engineering with the University of Science and Technology of China, Hefei, China. Her current research interests include distributed optimization in multi-agent systems, distributed energy management and demand response in smart grid.

Jiahu Qin (M'12-SM'18) received the first Ph.D. degree in control science and engineering from the Harbin Institute of Technology, Harbin, China, in 2012 and the second Ph.D. degree in systems and control from the Australian National University, Canberra, ACT, Australia, in 2014.

He is currently a Professor with the Department of Automation, University of Science and Technology of China, Hefei, China. His current research interests include multi-agent systems, cyber-physical systems, and complex dynamical networks.

Fangyuan Li (S'16-M'20) received the B.E. degree in electrical engineering and its automation from Southwest Jiaotong University, Chengdu, China, in 2014, and the Ph.D. degree in control science and engineering at the University of Science and Technology of China, Hefei, China, in 2019.

He is currently a Lecturer with the Department of Automation, Zhengzhou University, Zhengzhou, China. His research interests include distributed optimization and control in multi-agent systems and distributed energy management in smart grid.

Xinghuo Yu (M'92-SM'98-F'08) received the B.Eng. and M.Eng. degrees in electrical and electronic engineering from the University of Science and Technology of China, Hefei, China, in 1982 and 1984, and Ph.D. degree in control science and engineering from Southeast University, Nanjing, China in 1988, respectively.

He is an Associate Deputy Vice-Chancellor and a Distinguished Professor with RMIT University, Melbourne, VIC, Australia. He was also the President of IEEE Industrial Electronics Society for 2018 and 2019. His current research interests include control systems, complex and intelligent systems, and smart grids. He has served as an Associate Editor of IEEE Transactions on Automatic Control, IEEE Transactions on Circuits and Systems I: Regular Papers, IEEE Transactions on Industrial Electronics and IEEE Transactions on Industrial Informatics. He received a number of awards and honors for his contributions, including 2013 Dr.-Ing. Eugene Mittelmann Achievement Award of IEEE Industrial Electronics Society, 2018 M A Sargent Medal from Engineers Australia and 2018 Austalasian AI Distinguished Research Contribution Award from Australian Computer Society.

Yu Kang (M'09-SM'14) received the Dr. Eng. degree in control theory and control engineering from the University of Science and Technology of China, Hefei, China, in 2005. From 2005 to 2007, he was a Post-Doctoral Fellow with the Academy of Mathematics and Systems Science, Chinese Academy of Sciences, Beijing, China.

He is currently a Professor with the Department of Automation, University of Science and Technology of China. His current research interests include adaptive/robust control, variable structure control, mobile manipulator, and Markovian jump systems.